[DOI]10.12016/j.issn.2096-1456.202550566

·基础研究·

不同表面处理对3D打印氧化锆表面性状及即刻剪切粘接强度的影响

陈静，闫志琦，李佳乐，王富
口颌系统重建与再生全国重点实验室，国家口腔疾病临床医学研究中心，陕西省口腔医学重点实验室，空军军医大学第三附属医院修复科，陕西 西安（710032）

【摘要】 目的 研究不同表面处理方案对3D打印氧化锆表面性状及氧化锆-树脂即刻剪切粘接强度（shear bond strength，SBS）的影响，为临床操作提供参考。**方法** 应用3D打印技术制作两种不同表面的盘状氧化锆试件（直径14 mm，厚度1.2 mm），光滑表面组（S组）和微孔表面组（M组）每组40个，2组试件分别随机分为4个亚组分别进行表面处理：未处理（U组）、氧化铝喷砂（ST组）、氧化铝喷砂+Z-Prime瓷处理剂处理（ZP组）及氧化铝喷砂+Monobond N瓷处理剂处理（MN组）。对试件进行表面形貌观察、粗糙度测量，接触角测试评估润湿性。使用树脂水门汀将复合树脂柱（直径3.5 mm，高度2.0 mm）粘接于各组氧化锆试件表面，剪切试验测定即刻SBS，分析破坏模式。**结果** 扫描电镜下可明显看到S-U组宽度约2~5 μm的微沟槽结构以及M-U组直径400 μm的微孔结构，喷砂后S-ST组微沟槽结构被破坏，出现部分微裂纹，M-ST组微孔结构依旧清晰。相较于S-U、M-U组，喷砂后的氧化锆试件（S-ST组、S-ZP组、S-MN组、M-ST组、M-ZP组、M-MN组）的粗糙度显著提升，接触角明显减小。不同表面处理对3D打印氧化锆-树脂SBS具有显著影响，喷砂处理后（S-ST组、M-ST组）SBS显著高于未处理表面（S-U组、M-U组），联合应用瓷处理剂后（S-ZP组、S-MN组、M-ZP组、M-MN组）SBS进一步提高，但喷砂联合不同瓷处理剂对SBS的影响（S-ZP组 *vs.* S-MN组、M-ZP组 *vs.* M-MN组）无统计学差异；在相同表面处理时，微孔表面组（M-U组、M-ST组、M-MN组、M-ZP组）的SBS均显著高于光滑表面组（S-U组、S-ST组、S-MN组、S-ZP组）。**结论** 利用3D打印技术制备微孔表面能够提高树脂粘接效果，喷砂联合瓷处理剂可获得最高的即刻SBS。

【关键词】 增材制造氧化锆；表面处理；微孔结构设计；表面形貌；粗糙度；接触角；剪切粘接强度；机械嵌合；化学键合
【中图分类号】 R78 **【文献标志码】** A **【文章编号】** 2096-1456（2026）04-0328-10
【引用著录格式】 陈静，闫志琦，李佳乐，等. 不同表面处理对3D打印氧化锆表面性状及即刻剪切粘接强度的影响[J]. 口腔疾病防治, 2026, 34(4): 328-337. doi:10.12016/j.issn.2096-1456.202550566.

微信公众号

Effect of different surface treatments on the surface properties and immediate shear bond strength of 3D-printed zirconia

CHEN Jing, YAN Zhiqi, LI Jiale, WANG Fu. National Key Laboratory of Oral and Maxillofacial Reconstruction and Regeneration, National Clinical Research Center for Oral Diseases, Shaanxi Key Laboratory of Stomatology, Department of Prosthodontics, The Third Affiliated Hospital of Air Force Medical University, Xi'an 710032, China
Corresponding author: WANG Fu, Email: wangfu99@fmmu.edu.cn

【Abstract】 Objective To investigate the effect of different surface treatment protocols on the surface properties and immediate shear bond strength (SBS) between 3D-printed zirconia and resin cement to provide a reference for clinical practice. **Methods** Disc-shaped zirconia specimens (Ø 14 mm× 1.2 mm) with two different surface designs were

【收稿日期】2025-12-10；**【修回日期】**2026-02-12
【基金项目】国家自然科学基金（82371011）；国家口腔颌面重建与再生重点实验室开放研究基金（2024KB12）；陕西省卫生健康科研创新能力提升计划（2025TD-18）
【作者简介】陈静，医师，硕士研究生在读，Email：chenjing3656@163.com
【通信作者】王富，副教授，博士，Email：wangfu99@fmmu.edu.cn

fabricated using 3D printing technology: a smooth surface (Group S) and microporous surface (Group M), with 40 specimens in each group. Each group was further randomly divided into four subgroups according to surface treatment: untreated (Subgroup U), alumina sandblasting (Subgroup ST), alumina sandblasting + Z-Prime ceramic primer (Subgroup ZP), and alumina sandblasting + Monobond N ceramic primer (Subgroup MN). The surface morphology was examined, roughness was measured, and wettability was evaluated via contact-angle testing. Composite resin cylinders (Ø 3.5 mm× 2.0 mm) were bonded to the zirconia surfaces with resin cement. Immediate SBS was determined by shear testing, and failure modes were analyzed. **Results** Scanning electron microscopy revealed clear micro-grooves (2-5 μm wide) in Subgroup S-U and micropores (approximately 400 μm in diameter) in Subgroup M-U. After sandblasting, the micro-grooves in Subgroup S-ST were partially destroyed with some micro-cracks, while the microporous structure in Subgroup M-ST remained clear. Compared with Subgroups S-U and M-U, sandblasted zirconia specimens (Subgroups S-ST, S-ZP, S-MN, M-ST, M-ZP, M-MN) showed significantly increased roughness and decreased contact angles. Different surface treatments significantly affected SBS between 3D-printed zirconia and resin. Sandblasted groups (Subgroups S-ST and M-ST) had significantly higher SBS than untreated groups (Subgroups S-U and M-U). The application of ceramic primers after sandblasting (Subgroups S-ZP, S-MN, M-ZP, M-MN) further increased SBS; however, there was no statistically significant difference in SBS between the two primers used after sandblasting (Subgroup S-ZP *vs*. S-MN, Subgroup M-ZP *vs*. M-MN). Under the same surface treatment, microporous surface groups (Subgroups M-U, M-ST, M-MN, M-ZP) all exhibited significantly higher SBS than smooth surface groups (Subgroups S-U, S-ST, S-MN, S-ZP). **Conclusion** Fabricating a microporous surface using 3D printing technology can improve resin bonding effectiveness. Sandblasting combined with a ceramic primer yields the highest immediate SBS.

【Key words】 additive manufacturing zirconia; surface treatment; micropore structure design; surface topography; roughness; contact angle; shear bond strength; mechanical interlocking; chemical bonding

J Prev Treat Stomatol Dis, 2026, 34(4): 328-337.

【Competing interests】 The authors declare no competing interests.

This study was supported by the grants from the National Natural Science Foundation of China (No. 82371011), the Open Research Fund of the State Key Laboratory of Oral and Maxillofacial Reconstruction and Regeneration (No. 2024KB12), the Shaanxi Provincial Health Commission Innovation Capability Improvement Project (No. 2025TD-18).

氧化锆陶瓷因其卓越的机械强度、优异的生物相容性以及良好的美学性能，已成为口腔固定修复体如全冠、桥体及种植上部结构的主要材料[1-3]。然而，其高度化学稳定性及固有的低表面能导致表面活性较低，使其与树脂水门汀的粘接依旧面临挑战[4-5]。传统的表面处理手段主要包括机械喷砂、热酸蚀刻及化学硅涂层等[6]，喷砂处理通过物理方法增加表面粗糙度，但可能引入微裂纹并导致相变[7]；氢氟酸对硅酸盐类陶瓷有效，但对氧化锆几乎无蚀刻作用，处理效果有限[8-9]；硅涂层技术虽可通过形成Si-O-Si键提升化学结合力，但涂层与基底间热膨胀系数不匹配易导致界面剥离，限制其应用[10-12]。

当前，3D打印技术在口腔修复领域快速发展，先进喷墨定制（advanced customized jetting，ACJ）技术具备16.000 μm×17.625 μm的高分辨率及10 μm的层厚沉积能力[13]，对比研究数据表明，该技术在材料利用率及复杂几何拓扑结构的成型制备方面均显著优于传统加工方法[14-15]。尤为重要的是，ACJ技术利用其可精确构建微米级表面形貌的优势，如圆形、三形等微结构，可实现氧化锆表面形貌的精确设计，表面微结构设计不仅能增加粘接面积，还能引导树脂水门汀的渗透方向，形成更稳定的机械嵌合，为提高氧化锆-树脂的粘接效果提供了全新思路[16]。本研究团队前期建立3种圆形微孔分布密度和2种微孔深度，通过系列实验探究圆形微孔结构的深度和密度的设计对氧化锆-树脂粘接性能的影响，发现15%分布密度（微孔间距为500 μm）、深度40 μm、直径400 μm的圆形微结构能大幅度提升氧化锆的即刻剪切粘接强度（shear bond strength，SBS）[17]。然而，目前尚无研究系统探讨不同表面处理方式（如喷砂、专用瓷处理剂）对3D打印微结构氧化锆表面形貌、润湿性及剪切粘接强度（SBS）的影响。因此，本研究拟采用ACJ 3D打印技术制备具有标准化圆形微孔结构的氧化锆试件，进一步对比喷砂处理、不同瓷处理剂对其

表面形貌、表面能及剪切粘接强度(SBS)的作用差异，结合扫描电镜(scanning electron microscope，SEM)与破坏模式分析评估界面稳定性，旨在为临床优化氧化锆修复体的粘接策略提供科学依据与实验支持。

1　材料和方法

1.1　实验材料与设备

3D打印氧化锆(3Y-TZP，泰利斯，杭州)，组成成分如下：氧化锆(ZrO_2+Y_2O_3+HfO_2：99.2%)，其中氧化钇(Y_2O_3)占比5.50%，氧化铝(Al_2O_3)及其他氧化物小于1.0%；瓷处理剂Z-Prime Plus(Bisco，美国)和Monobond N(Ivoclar Vivadent，列支敦士登)；复合树脂(Te-Econom Plus，Ivoclar Vivadent，列支敦士登)；自粘接树脂水门汀(Multilink Speed，Ivoclar Vivadent，列支敦士登)；3D打印机(Carmel 1400，泰利斯，杭州)；牙科精细喷砂机(Basic classic No. 2945，Renfert GmbH，德国)，万能测试机(AG-10，岛津，日本)；扫描电镜(SU8010，日立，日本)；非接触式光学轮廓仪(ST 400，微纳科技，美国)；表面张力仪(Physics DCAT21，德菲，德国)。

1.2　3D打印氧化锆试件制备

应用3D打印技术制作2种具有不同表面的盘状氧化锆试件各40个，包括光滑表面组(S组)和微孔表面组(M组)，微孔直径为400 μm，以六边形方式紧密排列，孔间距500 μm，深度40 μm。3D打印机参数为：层厚10 μm，打印分辨率1 200 DPI。打印完成后按照制造商推荐方法移除支撑材料并行烧结处理[18]，最终成型尺寸为直径14 mm，厚度1.2 mm的盘状试件。所有试件无水乙醇超声清洗10 min，吹干备用。

1.3　氧化锆表面处理

将以上2组3D打印氧化锆试件分别随机分为4个亚组分别进行表面处理(n=10)。未处理(U组)：保持原打印表面；氧化铝喷砂(ST组)：使用粒径约50 μm的氧化铝颗粒在2.0 Bar气压下，距试件表面10 mm处垂直喷砂20 s，随后超声清洗；喷砂+Z-Prime(ZP组)：喷砂方式同ST组，超声清洗后，表面均匀涂布Z-Prime瓷处理剂，吹干；喷砂+Monobond N(MN组)：喷砂方式同ST组，超声清洗后，表面均匀涂布Monobond N瓷处理剂。

1.4　表面形貌观察及粗糙度测量

从所有亚组中分别选择3个代表性试件，经喷金处理后，采用扫描电镜进行表面微观形貌观察。同时使用非接触式光学轮廓仪进行表面形貌定量分析，实验参数设置为：扫描步长10 μm、扫描速度0.25 mm/s、采集频率100 Hz。每个试件随机选取5个测量点，取算术平均粗糙度(roughness average，Ra)作为该试件的表面粗糙度表征值。

1.5　接触角测试

采用动态表面张力仪进行接触角测试。在测试过程中，将10 μL去离子水滴均匀分布于试件表面，通过高精度成像系统实时捕捉液滴轮廓形态。随后采用Image J软件对捕获的液滴图像进行分析，测定接触角参数，取算术平均值作为该试件的接触角测量结果。

1.6　粘接试件制备

利用硅橡胶模具制备直径3.5 mm，高度为2.0 mm的复合树脂柱，使用自粘接复合树脂水门汀将复合树脂柱粘接于氧化锆试件表面，50 N恒定压力下固定，使用LED光固化灯(1 200 mW/cm^2)对边缘进行3 s预固化，清除多余树脂水门汀，再对各个面分别进行20 s光固化。所有粘接完成的试件立即转移至37 ℃恒温水浴箱中保持24 h。

1.7　即刻剪切粘接强度(SBS)测试

将粘接试件夹持于夹具并固定于万能试验机上进行SBS测试。加载力与粘接界面平行，加载速度为0.5 mm/min，直至粘接界面断裂，记录最大载荷F值(N)，剪切粘接强度(SBS)的计算公式为：P = F/S，P为剪切强度(MPa)，S为粘接面积(mm^2)。

1.8　破坏模式分析

SBS测试后，选取具有代表性的断裂面进行高分辨率扫描电子显微镜(SEM)观察，体式显微镜(×40)观察各组粘接试件破坏模式，分析不同模式占比，破坏模式分为3种：①粘接破坏：80%的损伤发生在氧化锆与粘接树脂的界面处，表现为氧化锆表面光滑且残留少量粘接剂(断裂的氧化锆圆盘表面未见树脂粘接剂残留)；②内聚破坏：80%的损伤发生在树脂内部(氧化锆圆盘表面几乎被树脂粘接剂完全覆盖)；③混合破坏：断裂同时涉及粘接破坏与内聚破坏(断裂的氧化锆圆盘表面可见部分残留树脂粘接剂)[18]。

1.9　统计学分析

采用SPSS 26.0统计软件对接触角、表面粗糙度及SBS数据进行系统分析。首先通过Shapiro-Wilk检验和Levene检验分别验证各参数的正态分布特性与方差齐性，采用双因素方差分析(Two-way ANOVA)对组间差异进行显著性检验，并通过

最小显著差异法(LSD)进行多重比较。所有统计分析均采用双侧检验,以α=0.05作为显著性判断阈值。

2　结　果

2.1　表面形貌特征

3D打印氧化锆光滑表面(S组)和微孔表面(M组)喷砂前后的扫描电镜下表面形貌如图1所示。可见喷砂前S-U组表面相对平滑,呈现出平行排列的周期性微沟槽结构(图1a),宽度约2~5 μm。喷砂后,S-ST组的微沟槽结构被破坏,出现部分微裂纹(图1b)。

喷砂前,M-U组可见直径为400 μm清晰的微孔结构,呈六边形分布,边界清晰(图1c)。喷砂处理后,M-ST组微孔结构仍清晰可见,未见明显的结构破坏,孔间区域可见微沟槽结构(图1d),表明3D打印氧化锆具有较好的结构稳定性。

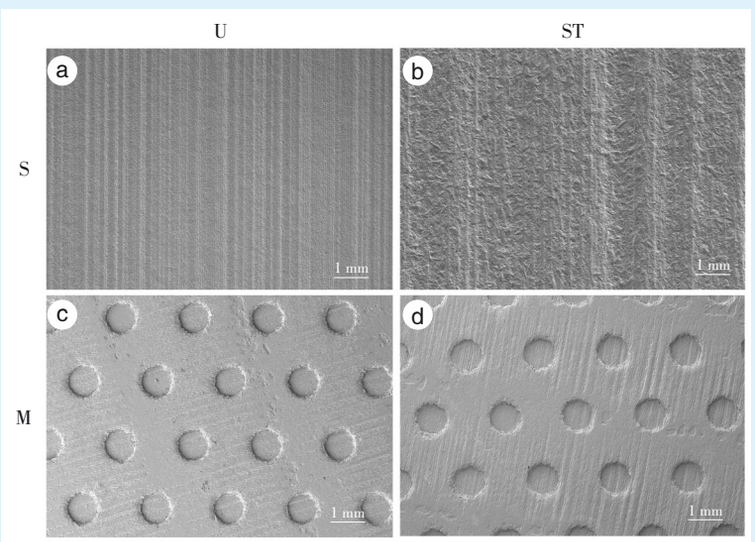

a: the smooth surface exhibited a relatively smooth surface with periodic microgrooves, even without a surface micropore design; b: the smooth surface after sandblasting retained periodic microgrooves with a few microcracks appearing; c: the microporous surface showed clearly distributed micropores (approximately 400 μm in diameter); d: the microporous surface after sandblasting demonstrated significant micropore structure stability, with cylindrical microstructures remaining intact and geometrically regular, and the periodic grooves were also preserved. S: smooth surface group; M: microporous surface group; U: untreated group, maintaining the original printed surface; ST: sandblasting treatment group

Figure 1　Surface morphology under a scanning electron microscope of 3D-printed zirconia specimens with different surface designs and after sandblasting

图1　不同表面设计及喷砂前后的3D打印氧化锆试件扫描电镜下表面形貌

2.2　粗糙度

喷砂后,氧化锆试件的粗糙度显著提升,具体见图2、表1。3D打印氧化锆的光滑表面S-U组并非完全光滑,可以看到周期性的微凹槽;经喷砂处理后,S-ST组Ra值相应升高;经喷砂联合瓷处理剂处理后,S-ZP组、S-MN组Ra值升高得更明显(图2a~2d)。

微孔表面M-U组可见清晰的直径为400 μm的微孔结构;喷砂处理后,M-ST组Ra值相应升高,经喷砂联合瓷处理剂处理后,M-ZP组、M-MN组Ra值反而降低(图2e~2h),表现出和光滑表面(S-ZP组、S-MN组)相反的Ra值趋势。

2.3　接触角

喷砂后,氧化锆试件的接触角显著降低,具体见图3、表2。不论是光滑表面或者微孔表面,对比S-U、M-U组,其喷砂后(S-ST组、M-ST组)氧化锆试件的接触角显著降低,对光滑表面或者微孔表面进行喷砂联合瓷处理剂处理后,S-ZP组、S-MN组、M-ZP组、M-MN组试件表现出与单纯喷砂处理后相似的接触角值。

2.4　即刻剪切粘接强度

光滑表面S-U组未进行处理时,SBS值最低:(9.98±2.23) MPa;喷砂处理使SBS值显著提升:S-ST组(15.48±0.94)MPa;联合应用瓷处理剂后,SBS

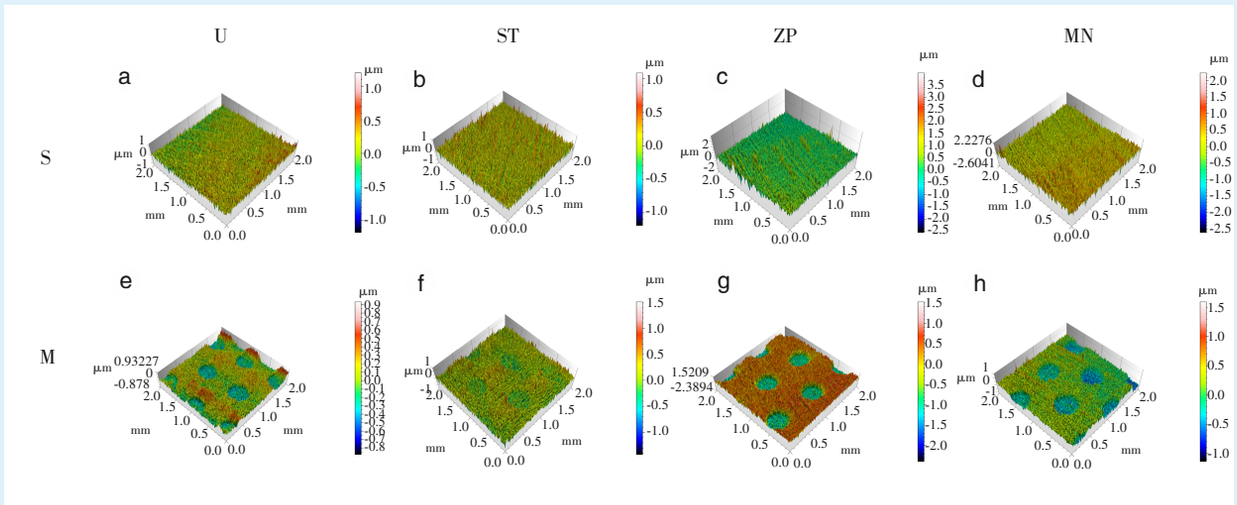

Compared with the smooth surface (a), the surface roughness of the zirconia specimens increased significantly after sandblasting (b), and the increase in surface roughness was more pronounced when sandblasting was combined with ceramic primer treatment (c & d). In contrast to the smooth surface group, compared with that of the microporous surface (e), the surface roughness after sandblasting (f) increased significantly, whereas it decreased instead when sandblasting was combined with ceramic primer treatment (g & h). S: smooth surface group; M: microporous surface group; U: untreated group, maintaining the original printed surface; ST: sandblasting treatment group; ZP: sandblasting + Z-Prime treatment group; MN: sandblasting + Monobond N treatment group

Figure 2　Three-dimensional morphology under a scanning electron microscope of 3D-printed zirconia specimens after different surface treatments

图2　不同表面处理后的3D打印氧化锆试件扫描电镜下三维形貌图

表1　不同表面处理后的3D打印氧化锆试件表面粗糙度(Ra)

Table 1　Surface roughness (Ra) of 3D-printed zirconia specimens after different surface treatments　　μm, $\bar{x}\pm s$

Group	Surface treatment				*F*	*P*
	U	ST	ZP	MN		
S group	0.16±0.01^{a}	0.25±0.07^{ab}	0.44±0.11^{c}	0.31±0.04^{bc}	2.951 9	<0.001
M group	0.30±0.10^{a}	0.64±0.11^{b}	0.45±0.07^{c}	0.35±0.07^{ac}	2.829 7	<0.001
F	10.828 6	45.201 5	0.020 8	0.320 7	–	–
P	0.007 2	< 0.000 1	0.765 7	0.419 0	–	–

Ra means arithmetic mean roughness. Within the same row, statistically significant ($P < 0.05$) between-group differences are represented by different lowercase letters. S: smooth surface group; M: microporous surface group; U: untreated group, maintaining the original printed surface; ST: sandblasting treatment group; ZP: sandblasting + Z-Prime treatment group; MN: sandblasting + Monobond N treatment group

值进一步提升,且两种瓷处理剂间无统计学差异:S-ZP组(21.37±2.00) MPa,S-MN组(21.94±1.77) MPa。微孔表面表现出相似的趋势,未进行处理的微孔表面M-U组SBS值最低:(17.68±1.52)MPa;喷砂处理显著提升SBS值:M-ST组(22.12±1.83)MPa;联合应用瓷处理剂后,SBS值进一步提升:M-ZP组(23.92±2.13)MPa,M-MN组(26.51±3.59)MPa,且两种瓷处理剂之间无统计学差异。

在相同表面处理的情况下,微孔表面组的即刻SBS均显著高于光滑表面组。微孔表面经喷砂联合应用瓷处理剂处理后,可获得最高的即刻SBS值:M-ZP组(23.92±2.13) MPa,M-MN组(26.51±3.59)MPa(图4)。

2.5　破坏模式

图5展示了3种典型破坏模式的微观形貌:粘接破坏(adhesive failure)(图5a):氧化锆表面光滑,仅残留少量树脂水门汀,界面分离主要发生在氧化锆与树脂的接触面,此模式常见于未处理组(S-U组和M-U组)以及单纯喷砂组(S-ST组和M-ST组),表明界面化学键合不足。内聚破坏(cohesive failure)(图5b):氧化锆表面几乎完全被树脂覆盖,断裂发生在树脂内部,说明界面结合强度高于树

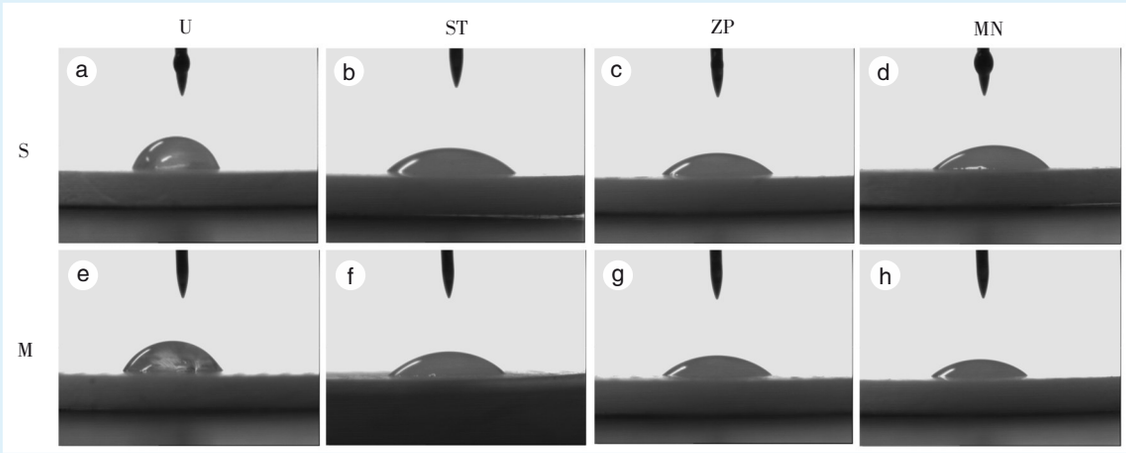

Compared with the smooth surface (a), after sandblasting, the contact angle of the zirconia surface significantly decreased (b). However, the combination of sandblasting and ceramic primer (Z-Prime or Monobond) treatment had no significant effect on the contact angle of the zirconia surface (c & d). The microporous surface showed a similar trend to the smooth surface (e-h). S: smooth surface group; M: microporous surface group; U: untreated group, maintaining the original printed surface; ST: sandblasting treatment group; ZP: sandblasting + Z-Prime treatment group; MN: sandblasting + Monobond N treatment group

Figure 3　Images of 3D-printed zirconia specimens contact angle tests after different surface treatments

图3　不同表面处理后的3D打印氧化锆试件接触角试验图像

表2　不同表面处理后的3D打印氧化锆试件表面接触角

Table 2　Surface contact angles of 3D-printed zirconia specimens after different surface treatments　°, $\bar{x}\pm s$

Group	Surface treatment				*F*	*P*
	U	ST	ZP	MN		
S group	76.67±1.72^{a}	47.94±1.23^{b}	46.93±0.31^{b}	45.36±0.40^{b}	190.399 2	<0.001
M group	61.13±0.70^{a}	46.76±0.85^{b}	46.27±1.34^{b}	45.53±1.01^{b}	55.685 3	<0.001
F	28.254 1	6.020 3	1.156 8	0.215 9	–	–
P	0.013 8	0.241 3	0.988 2	> 0.999 9	–	–

Within the same row, statistically significant (P<0.05) between-group differences are represented by different lowercase letters. S: smooth surface group; M: microporous surface group; U: untreated group, maintaining the original printed surface; ST: sandblasting treatment group; ZP: sandblasting + Z-Prime treatment group; MN: sandblasting + Monobond N treatment group

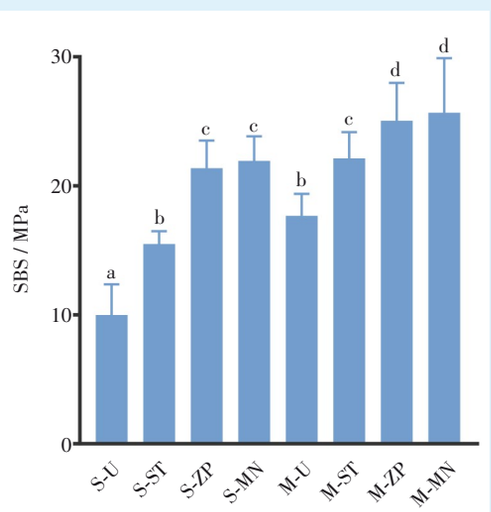

SBS was lowest in the S-U group. Sandblasting significantly increased SBS (S-ST group). The combined application of ceramic treatment agents further improved SBS, with no statistical difference between the two ceramic treatment agents (S-ZP and S-MN groups). The microporous surface groups (M-U, M-ST, M-ZP, and M-MN groups) showed a similar trend of improved SBS. The same superscript lowercase letters indicate $P > 0.05$, while different superscript lowercase letters indicate $P < 0.05$. S: smooth surface group; M: microporous surface group; U: untreated group, maintaining the original printed surface; ST: sandblasting treatment group; ZP: sandblasting + Z-Prime treatment group; MN: sandblasting + Monobond N treatment group; SBS: shear bond strength

Figure 4　Immediate SBS of 3D-printed zirconia specimens with different surface treatments

图4　不同表面处理的3D打印氧化锆试件即刻剪切粘接强度

脂自身强度。混合破坏(mixed failure)(图5c):氧化锆表面部分区域残留树脂,同时伴随界面剥离和内聚断裂,是机械嵌合与化学键合协同作用的结果。无论在光滑表面或者微孔表面,应用喷砂联合瓷处理剂处理后,如S-ZP组、S-MN组、M-ZP组和M-MN组中均以混合破坏占比显著。对于光滑表面,未处理组(S-U组)和喷砂组(S-ST组)粘接破坏和混合破坏均超过40%,而喷砂联合瓷处理剂处理后,S-ZP组和S-MN组粘接破坏比例显著降低,混合破坏显著提升,均达到80%;对于微孔表面,未处理组(M-U组)和喷砂组(M-ST组)混合破坏占比均超过50%,喷砂联合应用瓷处理剂处理后,M-ZP组和M-MN组粘接破坏比例显著降低至20%,混合破坏占比超过80%(图6)。

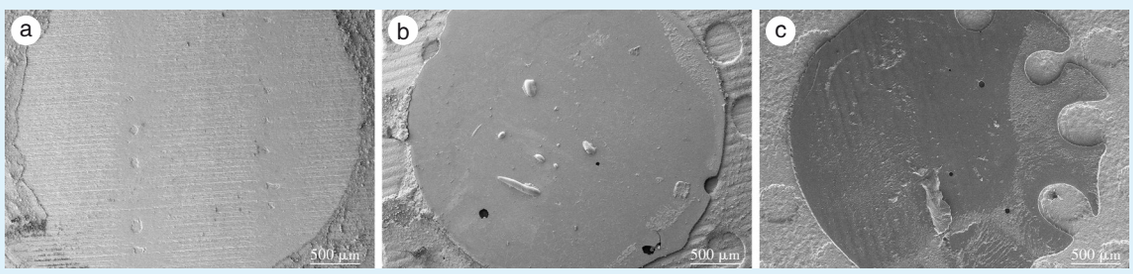

a: the zirconia surface appeared smooth with a small amount of adhesive residue (adhesive failure); b: the zirconia surface was almost completely covered by resin adhesive (cohesive failure); c: partial residual resin adhesive was visible on the fractured zirconia disk surface (mixed failure). SEM: scanning electron microscope

Figure 5　SEM analysis of fracture types in 3D-printed zirconia-resin specimens

图5　3D打印氧化锆-树脂试件破坏类型SEM分析

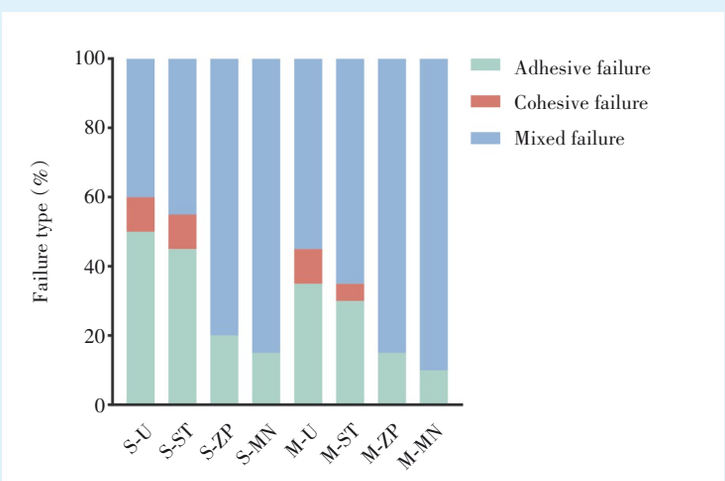

For the smooth surfaces, the S-U and S-ST groups primarily exhibited adhesive failure and mixed failure, whereas after applying ceramic primers (S-ZP and S-MN groups), the proportion of adhesive failure significantly decreased. For microporous surfaces, mixed failure was predominant in the M-U and M-ST groups, and after applying ceramic primers (M-ZP and M-MN groups), the proportion of adhesive failure also significantly decreased. S: smooth surface group; M: microporous surface group; U: untreated group, maintaining the original printed surface; ST: sandblasting treatment group; ZP: sandblasting + Z-Prime treatment group; MN: sandblasting + Monobond N treatment group

Figure 6　Analysis of the failure types of 3D-printed zirconia-resin specimens

图6　3D打印氧化锆-树脂试件破坏类型分析

3　讨　论

在口腔修复领域,增材制造技术展现出显著优势,尤其在材料利用率和复杂结构成型方面表现突出[19-20]。ACJ技术,又称为纳米颗粒喷射技术,作为直接喷墨技术(direct ink printing, DIP)的改进版本,其采用双墨系统(氧化锆部件专用油墨

与支撑结构油墨）实现10 μm超薄层厚[13, 21]，能够高精度制造具有复杂几何特征的氧化锆修复体。研究表明，ACJ法制备的全解剖氧化锆冠相较于传统减材制造工艺，在边缘密合度和表面粗糙度等关键指标上具有显著优势[22-23]。与数字光处理（digital light processing，DLP）等增材技术相比，ACJ成型的氧化锆冠具有更高的尺寸精度和临床适应性。Yoon等[24]证实激光蚀刻的蜂窝状纹理可通过增加树脂微机械嵌合面积使粘接强度提升，但该技术存在20 μm热损伤层和低加工效率等固有缺陷[25-26]。本研究采用ACJ技术构建表面微孔拓扑结构氧化锆，通过系统比较不同表面处理方案发现：微孔结构（直径400 μm，深度40 μm）结合喷砂+Monobond N瓷处理剂处理可使即刻SBS较光滑表面显著提升，其增强机制源于微孔结构产生的机械嵌合效应与瓷处理剂形成的化学键协同作用。

3.1　表面形貌设计增强机械嵌合

表面形貌是粘接界面的物理基础[27]，3D打印氧化锆表面周期性分布的微沟槽结构（宽度2~5 μm），以及微孔结构对粘接性能的提升具有重要影响，表1数据显示，微孔表面未处理组（M-U组）的粗糙度Ra为（0.30±0.10）μm，显著高于光滑表面组S-U组Ra（0.16±0.01）μm，意味着3D打印微孔表面提供了更大的比表面积，增大了机械嵌合位点，从而显著增强界面结合力[28-29]。喷砂处理后，两组表面形貌均保持高度稳定性，特别是微孔表面组（M-ST组、M-ZP组、M-MN组）仍维持完整的微孔结构，这对维持粘接界面的长期稳定性至关重要[30]。即刻SBS数据进一步证实了该结论：即使未经任何表面处理，微孔表面组的SBS亦显著高于光滑表面组（M-U组17.68 MPa *vs.* S-U组9.98 MPa），充分证明表面微结构有效增强了机械锁合作用，为粘接提供了可靠的物理支撑[31]。

3.2　喷砂处理通过粗糙化与活化表面改善浸润与锚定

喷砂和酸蚀是陶瓷修复材料常见的两种表面处理方法[32-33]，然而，由于氧化锆本身不存在玻璃相，常规酸蚀无明显效果[34]。对于氧化锆修复体而言，喷砂能有效增加表面粗糙度[35]，尽管有文献指出单纯机械处理无法显著提高剪切粘接强度（SBS）[36]，但本研究发现对于3D打印表面，特定条件的喷砂可提高SBS。这种不同的结果差异可能源于以下几方面：首先，ACJ打印氧化锆表面固有微沟槽结构为喷砂提供了优化的基底，喷砂后在保留周期性结构的同时引入多级粗糙度，产生协同效应；微孔表面的设计放大喷砂效果，显著提升树脂与表面的机械嵌合。

喷砂处理后表面粗糙度Ra值明显升高，光滑表面粗糙度从（0.16±0.01）μm（S-U组）升至（0.25±0.07）μm（S-ST组），微孔表面从（0.30±0.10）μm（M-U组）升至（0.64±0.11）μm（M-ST组），这种多级粗糙结构为树脂渗透提供了更优路径。接触角是评价表面润湿性的指标，较低的接触角表示更好的亲水性，利于粘接剂铺展和化学键合[37-38]。接触角测试显示喷砂后接触角急剧下降（S组从76.67°降至47.94°，M组从61.13°降至46.76°），这种变化利于粘接剂（如树脂）在氧化锆表面的均匀铺展，减少界面缺陷，并促进化学键合（如通过偶联剂的磷酸基团或硅烷基团），这可能是喷砂组（S-ST组、M-ST组）氧化锆SBS提高的主要原因之一。

未经过表面处理时，微孔表面组的接触角明显低于光滑表面组（M-U组61.13°±0.70° *vs.* S-U组76.67°±1.72°），说明表面拓扑结构进一步增强了润湿性，结合即刻SBS，喷砂组（S-ST组15.48 MPa和M-ST组22.12 MPa）强度显著高于抛光组（S-U组9.98 MPa和M-U组17.68 MPa），微孔表面喷砂后M-ST组粗糙度（0.64±0.11）μm远高于光滑表面S-ST组（0.25±0.07）μm，且接触角均一化（约47°），说明喷砂在微结构基础上进一步优化了浸润均匀性，降低局部粘接缺陷的发生率。

3.3　瓷处理剂通过化学键合提升界面稳定性

含磷酸酸性单体10-甲基丙烯酰氧基癸基二氢磷酸酯（10-MDP）的处理剂或粘接剂因其能与氧化锆表面形成化学键而被广泛认可[36, 39]，因此，喷砂后涂布含10-MDP处理剂或树脂的联合处理方案常作为氧化锆粘接的推荐程序[18, 39-40]。本研究结果显示，喷砂联合瓷处理剂处理后使接触角进一步降低（如S-ZP组46.93°，S-MN组45.36°），但变化幅度小于喷砂作用，说明其主要作用为化学修饰而非物理形变。喷砂联合瓷处理剂处理后，剪切强度达到峰值（M-ZP组23.92 MPa，M-MN组26.51 MPa），且破坏模式中粘接破坏比例显著下降，证明化学键合有效提高粘接界面质量。破坏模式分析表明：未经处理的光滑表面组（S-U组）的粘接破坏比例较高（达50%），而喷砂联合瓷处理剂处理后（S-ZP组、S-MN组）混合破坏比例升至80%。微孔表面组（M组）的混合破坏占比普遍高于光滑表面（M-MN组达85%），喷砂联合瓷处理剂

进行表面处理显著降低了粘接破坏比例(S-MN组较S-U组下降约40%),M-MN组粘接破坏仅占10%,凸显了微孔设计对粘接质量的贡献。为更好地模拟临床实践,本研究采用喷砂+含10-MDP瓷处理剂作为对比标准,结果表明,表面微孔设计的粘接性能要显著优于光滑表面。

最高粘接强度出现在M组喷砂联合瓷处理剂处理后(M-ZP组23.92 MPa和M-MN组26.51 MPa),粘接强度提升的机制主要包括以下方面:表面形貌设计为粘接提供宏观的物理基础,增加机械嵌合位点、增加粘接面积[29];喷砂在微观尺度优化粗糙度与润湿性,提高高分子材料在氧化锆表面的铺展[38];瓷处理剂中的10-MDP分子可与氧化锆形成P-O键合,强化粘接界面的稳定性[36, 39],三者交互影响,共同提升3D打印氧化锆的即刻SBS。综上所述,优化表面形貌设计结合适当表面处理(喷砂+瓷处理剂),可通过"机械嵌合-化学键合"双重机制,系统性提升氧化锆粘接强度,对于提升临床氧化锆修复体的粘接效果具有重要的应用价值。

【Author contributions】 Chen J performed the experiments, analyzed the data and wrote the paper. Yan ZQ and Li JL were responsible for results collection and data analysis. Wang F designed the study and revised the article. All authors read and approved the final manuscript as submitted.

参考文献

[1] Han MK. Advances and challenges in zirconia-based materials for dental applications[J]. J Korean Ceram Soc, 2024, 61(5): 783-799. doi: 10.1007/s43207-024-00416-7.

[2] Thirumalaivasan N, Nangan S, Verma D, et al. Exploring the diverse nanomaterials employed in dental prosthesis and implant techniques: an overview[J]. Nanotechnol Rev, 2025, 14: 20250140. doi: 10.1515/ntrev-2025-0140.

[3] Yang Y, Hu C, Liu Q, et al. Research progress and prospects of colored zirconia ceramics: a review[J]. J Adv Ceram, 2024, 13(10): 1505-1522. doi: 10.26599/JAC.2024.9220941.

[4] Chen X, Yu C, Hua L, et al. Nonthermal atmospheric plasma promotes bonding between adhesive monomers and zirconia[J]. J Esthet Restor Dent, 2025, 37(4): 950-959. doi: 10.1111/jerd.13338.

[5] 张颖, 胡丹丹, 黄皓宁, 等. 高半透性氧化锆基底的不同处理对锆-瓷结合强度的影响[J]. 口腔疾病防治, 2021, 29(7): 456-461. doi: 10.12016/j.issn.2096-1456.2021.07.004.
Zhang Y, Hu DD, Huang HN, et al. Effect of different treatments of highly translucent zirconia on the bonding strength between zirconia and veneering porcelain[J]. J Prev Treat Stomatol Dis, 2021, 29(7): 456-461. doi: 10.12016/j.issn.2096-1456.2021.07.004.

[6] Srinivasan G, Manickam A, Sivakumar S, et al. A comprehensive review: surface modification strategies to enhance corrosion resistance of zirconia-based biomaterials in implant applications[J]. J Mater Sci Mater Eng, 2025, 20(1): 76. doi: 10.1186/s40712-025-00294-9.

[7] Pantea M, Ciocan LT, Vasilescu VG, et al. Effects of different surface treatments and accelerated aging on dental zirconia: an *in vitro* study[J]. J Funct Biomater, 2025, 16(7): 263. doi: 10.3390/jfb16070263.

[8] Nishizawa Y, Kawamoto T, Ikeda H. Bonding pretreatment of aesthetic dental CAD-CAM materials through surface etching with a mixed aqueous solution of ammonium fluoride and ammonium hydrogen sulfate[J]. J Funct Biomater, 2024, 15(3): 71. doi: 10.3390/jfb15030071.

[9] Abdelraouf RM, Tsujimoto A, Hamdy TM, et al. The effect of surface treatments of presintered zirconia on sintered surfaces[J]. J Compos Sci, 2023, 7(9): 396. doi: 10.3390/jcs7090396.

[10] Kern M. Bonding to oxide ceramics-laboratory testing versus clinical outcome[J]. Dent Mater, 2015, 31(1): 8-14. doi: 10.1016/j.dental.2014.06.007.

[11] Grasel R, Santos MJ, Rêgo HC, et al. Effect of resin luting systems and alumina particle air abrasion on bond strength to zirconia[J]. Oper Dent, 2018, 43(3): 282-290. doi: 10.2341/15-352-L.

[12] Vitti RP, Catelan A, Amaral M, et al. Zirconium in dentistry [M]// Advanced Dental Biomaterials. Amsterdam: Elsevier, 2019: 317-345.

[13] Zhang F, Spies BC, Willems E, et al. 3D printed zirconia dental implants with integrated directional surface pores combine mechanical strength with favorable osteoblast response[J]. Acta Biomater, 2022, 150: 427-441. doi: 10.1016/j.actbio.2022.07.030.

[14] Lyu J, Yang X, Li Y, et al. Effect of build angle on the dimensional accuracy of monolithic zirconia crowns fabricated with the nanoparticle jetting technique[J]. J Prosthet Dent, 2023, 130(4): 613.e1-613.e8. doi: 10.1016/j.prosdent.2023.07.025.

[15] Zhong S, Shi Q, Deng Y, et al. High-performance zirconia ceramic additively manufactured *via* nanoparticle jetting[J]. Ceram Int, 2022, 48(22): 33485-33498. doi: 10.1016/j.ceramint.2022.07.294.

[16] Liu L, Zhang J, Zhu L, et al. The effect of surface texture on the bonding performance of zirconia fabricated by nanoparticle jetting additive manufacturing[J]. Ceram Int, 2025, 51(1): 1-8. doi: 10.1016/j.ceramint.2024.10.030.

[17] Chen J, Yan Z, Tang K, et al. Micropore texture design enhancing zirconia-resin bonding of additively manufactured zirconia[J]. Surf Interfaces, 2025, 77: 108008. doi: 10.1016/j.surfin.2025.108008.

[18] Jin C, Wang J, Huang Y, et al. Effects of hydrofluoric acid concentration and etching time on the bond strength to ceramic-coated zirconia[J]. J Adhes Dent, 2022, 24: 125-136. doi: 10.3290/j.jad.b2838165.

[19] Baumgartner S, Gmeiner R, Schönherr JA, et al. Stereolithography-based additive manufacturing of lithium disilicate glass ceramic for dental applications[J]. Mater Sci Eng C Mater Biol Appl, 2020, 116: 111180. doi: 10.1016/j.msec.2020.111180.

[20] Ye Z, Zhu L, Zhou T, et al. Shear bond strength, finite element analysis, flexural strength and accuracy analysis of additively manufactured bio-inspired 3Y-TZP for dental applications[J]. J Mater Res Technol, 2024, 29: 4588-4596. doi: 10.1016/j.

jmrt.2024.02.164.

[21] Li M, Huang S, Willems E, et al. UV-curing assisted direct ink writing of dense, crack-free, and high-performance zirconia-based composites with aligned alumina platelets[J]. Adv Mater, 2024, 36(5): e2306764. doi: 10.1002/adma.202306764.

[22] Camargo B, Willems E, Jacobs W, et al. 3D printing and milling accuracy influence full-contour zirconia crown adaptation[J]. Dent Mater, 2022, 38(12): 1963-1976. doi: 10.1016/j.dental.2022.11.002.

[23] Rues S, Zehender N, Zenthöfer A, et al. Fit of anterior restorations made of 3D-printed and milled zirconia: an *in-vitro* study[J]. J Dent, 2023, 130: 104415. doi: 10.1016/j.jdent.2023.104415.

[24] Yoon JY. Improving zirconia – resin cement bonding through laser surface texturing: a comparative study[J]. Prosthesis, 2025, 7(1): 19. doi: 10.3390/prosthesis7010019.

[25] Morales M, García-González S, Plch M, et al. Laser machining of nickel oxide – yttria stabilized zirconia composite for surface modification in solid oxide fuel cells[J]. Crystals, 2023, 13(7): 1016. doi: 10.3390/cryst13071016.

[26] Zhang Y, Wei C, Fukui T, et al. Ultrafast processing of zirconia ceramics by transient and selective laser absorption[J]. Ceram Int, 2024, 50(14): 25273-25281. doi: 10.1016/j.ceramint.2024.04.257.

[27] Sundfeld Neto D, Naves LZ, Costa AR, et al. The effect of hydrofluoric acid concentration on the bond strength and morphology of the surface and interface of glass ceramics to a resin cement[J]. Oper Dent, 2015, 40(5): 470-479. doi: 10.2341/14-133-L.

[28] Dewan H. Clinical effectiveness of 3D-milled and 3D-printed zirconia prosthesis-a systematic review and meta-analysis[J]. Biomimetics, 2023, 8(5): 394. doi: 10.3390/biomimetics8050394.

[29] Monteiro RV, Dos Santos DM, Bernardon JK, et al. Effect of surface treatment on the retention of zirconia crowns to tooth structure after aging[J]. J Esthet Restor Dent, 2020, 32(7): 699-706. doi: 10.1111/jerd.12623.

[30] Zicari F, Monaco C, Cardoso MV, et al. Bonding effectiveness of veneering ceramic to zirconia after different grit-blasting treatments[J]. Dent J , 2024, 12(7): 219. doi: 10.3390/dj12070219.

[31] Abdou A, Hussein N, Abd El-Sattar NEA, et al. MDP-salts as an adhesion promoter with MDP-primers and self-adhesive resin cement for zirconia cementation[J]. BMC Oral Health, 2023, 23(1): 907. doi: 10.1186/s12903-023-03663-y.

[32] Neis CA, Albuquerque NL, Albuquerque Ide S,et al. Surface treatments for repair of feldspathic, leucite- and lithium disilicate-reinforced glass ceramics using composite resin[J]. Braz Dent J, 2015, 26(2): 152-155. doi: 10.1590/0103-6440201302447.

[33] Turunç-Oğuzman R, Şişmanoğlu S. Influence of surface treatments and adhesive protocols on repair bond strength of glass-matrix and resin-matrix CAD/CAM ceramics[J]. J Esthet Restor Dent, 2023, 35(8): 1322-1331. doi: 10.1111/jerd.13131.

[34] Sales A, Rodrigues SJ, Mahesh M, et al. Effect of different surface treatments on the micro-shear bond strength and surface characteristics of zirconia: an *in vitro* study[J]. Int J Dent, 2022, 2022: 1546802. doi: 10.1155/2022/1546802.

[35] Okada M, Taketa H, Torii Y, et al. Optimal sandblasting conditions for conventional-type yttria-stabilized tetragonal zirconia polycrystals[J]. Dent Mater, 2019, 35(1): 169-175. doi: 10.1016/j.dental.2018.11.009.

[36] Al-Amari AS, Saleh MS, Albadah AA, et al. A comprehensive review of techniques for enhancing zirconia bond strength: current approaches and emerging innovations[J]. Cureus, 2024, 16(10): e70893. doi: 10.7759/cureus.70893.

[37] Wongsue S, Thanatvarakorn O, Prasansuttiporn T, et al. Effect of surface topography and wettability on shear bond strength of Y-TZP ceramic[J]. Sci Rep, 2023, 13(1): 18249. doi: 10.1038/s41598-023-45510-8.

[38] Petrov AE, Bakeev IY, Zenin AA, et al. Effect of electron beam treatment of composite ATZ and TZP ceramics on surface topography and reaction of osteoblast-like cells[J]. J Surf Investig, 2024, 18(6): 1656-1661. doi: 10.1134/S1027451024701672.

[39] Nagaoka N, Yoshihara K, Feitosa VP, et al. Chemical interaction mechanism of 10-MDP with zirconia[J]. Sci Rep, 2017, 7: 45563. doi: 10.1038/srep45563.

[40] 赵莉, 赵克. 不同功能成分底涂剂对氧化锆耐久粘接强度的影响[J]. 口腔疾病防治, 2024, 32(7): 502-508. doi: 10.12016/j.issn.2096-1456.2024.07.003.
Zhao L, Zhao K. Effect of various primers on the long-term bond strength to zirconia[J]. J Prev Treat Stomatol Dis, 2024, 32(7): 502-508. doi: 10.12016/j.issn.2096-1456.2024.07.003.

（编辑　张琳）

官网